Tensile and Fatigue Properties of SiC Whiskers and SiC Particulate Reinforced Aluminum Composites

CHITOSHI MASUDA and YOSHIHISA TANAKA
National Research Institute for Metals, 12–3–2, Nakameguro, Meguro-ku, Tokyo, Japan

Abstract

Tensile and fatigue properties were evaluated for two commercially fabricated aluminum alloy matrix composites containing SiC whiskers or SiC particles. Tensile strength of SiCw/Al2024 composite could be predicted by the equation proposed by Fukuda et al. The fatigue strength for the volumefraction of Vf= 0.3 was also estimated to be comparable or superior to that of annealed Ti-6Al-4V alloy fabricated by powder metallurgy. For SiCp/A356 composite the tensile strength and fatigue strength increased with increasing the volume fraction of SiC particles at the volume fraction of Vf=0.1, while those values tended to saturate or decreased at Vf=0.2. In order to improve the fatigue strength, it would be necessary to reduce the shrinkage introduced during the casting process which causes fish eye fatigue crack origins.

1. Introduction

The majority of effort in aluminum matrix composites has been directed toward the development of high performance composites, with very high strength and moduli. It has been reported that tensile strength[1)-7)] and fatigue strength[7)] of whiskers reinforced aluminum composites were superior to those of matrix alloys, while tensile ductility[1),3),4),6)] and fracture toughness[1),4)] of those composites were very lower than those of matrix alloys. The tensile strength of aluminum composites reinforced by SiC particulates were comparable to or higher than that for aluminum composites reinforced by SiC whiskers[6),7)]. On the other hand, fatigue strength at 10^7 cycles was about 50-70% higher for 6061 and 7075 aluminum composites reinforced by 20%- or 15%-SiC whiskers than that those matrix alloys[7)]. Fatigue crack propagation rates were about one order magnitude lower for 6061 aluminum composite reinforced by 20%-SiC whiskers than those for matrix alloy in the direction transverse to aligned whiskers[7)]. It is suggested that the increase of fatigue strength would cause by the effect of whiskers on the fatigue crack arrest or stoppage.

In this study the tensile and fatigue properties were evaluated and fracture mechanisms were discussed for SiC whiskers or SiC particulate reinforced aluminum composites in comparison to the steels and titanium

alloys.

2. Experimental procedures

Two types of composites were used in this study. One was SiC whisker reinforced composite (SiCw/Al2024), the other was SiC particulate reinforced composite (SiCp/A356). The volume fraction of SiC whiskers was 0.1 for SiCw/Al2024 composite and for SiCp/A356 composite the volume fraction was 0.1 and 0.2. Composite SiCw/Al2024 was made by Tokai Carbon Co. Ltd.. The whiskers were β-SiC with diameter ranging 0.1 to 1.0 μm and original lengths up to 15 μm. Al2024 composites reinforced by 10%-SiC whiskers were fabricated by powder metallurgy and the billet was extruded to the form bar. The extrusion ratio was about 10. The SiCp/A356 composites were fabricated by casting method by Dural Aluminum Composite Corporation. Unreinforced aluminum alloy AC4CH was also used in this study to obtain the reference data to A356 alloy.

The specimens was heat-treated under a T6 condition. Tensile tests were conducted on round tensile specimens 140mm long with 50 mm long reduced section, 10 mm diameter. Tensile speed was 0.5 mm per minutes up to the 0.2 % yield stress and then 2 mm per minutes until failure. Fatigue tests were performed on round specimens 130 mm long with 20mm long reduction section, 6 mm in diameter under the rotating bending conditions (50Hz) in air.

3. Results and discussions

3.1 Microstructures

Figure 1 shows the microstructures of these composites. In the Fig. 1(a) silicon carbide is poor in the light areas, while silicon carbide is rich in the dark areas. This figure exhibits that there are regions with higher silicon carbide content. For SiC particle reinforced aluminum composite SiC particles are also heterogeneously distributed in the matrix as shown in Fig. 1(b) and (c). A observation at high magnification revealed that the SiC particles were triangular or square and those average sizes are larger for Vf=0.2 than for Vf=0.1 of SiCp/A356 composites. It is considered that it would be difficult to disperse the smaller particle in the molten.

3.2 Tensile properties

Tensile properties for T6 conditions and as received conditions are given in Table 1. Figure 2 shows the relationship between the tensile strength and the volume fraction for aluminum composites reinforced by SiC whiskers or SiC particulates. Reference data also plotted in the same figure. The straight line was given the tensile strength estimated by equation (1)and (2)[8].

$$\sigma c = \sigma w Vf F(lc/l) Co + \sigma m (1-Vf) \qquad (1)$$

$$F(lc/l) = 1 - lc/2l \quad (lc > l)$$

$$= l/2lc \quad (lc < l)$$

$$lc/d = \sigma w / \sigma m \qquad (2)$$

Where σc, σw, and σm are the tensile strength of composite, whiskers and matrix, Vf is the volume fraction, F(lc/l) is the factor of fiber length and Co is the fiber orientation factor. lc and l denote fiber critical length and average length. d is the diameter of whiskers. The value of 13.7GPa(value as shown in catalogue) was used for the strength of SiC whiskers, σw, while σm was about 480MPa. In order to examine the whiskers diameter and length, the specimen was etched as shown in Fig.3. The average values d and l were about

0.57 and 4.70μm in this study. The value of lc calculated from eq. (2) was about 14μm. Then F(lc/l) is l/2lc. The value of σc estimated was about 630MPa at the volume fraction of 0.1. This value is equivalent to the experimental one of 640MPa.

3.3 Fatigue properties

Stress-Number of cycles to failure diagram showing rotating bending fatigue properties of composites is given in Fig. 4. In the figures the lines are estimated by the regression method for SiCw/Al2024 and SiCp/A356 composites on the semi-logarithm paper. For SiCw/Al2024 composite and AC4CH aluminum alloy the fatigue limit is clearly found, while for SiCp/A356 composites the fatigue limit is not seen in the range up to 10^7 cycles. The fatigue strength at 10^7 cycles was for SiCw/Al2024 composite higher than that for Al2024 alloy fabricated by powder metallurgy[9]. On the other hand, for SiCp/A356 composites at the volume fraction of 0.1 the fatigue strength was higher than that for AC4CH aluminum alloy, while at the volume fraction of 0.2 the fatigue strength was equivalent to that of AC4CH alloy. The values of fatigue strength estimated are also given in Table 2.

The fatigue strength at 10^7 cycles for the composites was related to the ultimate tensile strength as shown in Fig. 5. In the same figure the enclosed region indicates the data for high temperature tempered martensitic(HTTM) steels. For aluminum composites reinforced by SiC whiskers and SiC particulates the linear relationship is also found between the fatigue strength, σ_{cw}, and tensile strength, σ_B, described by equation (3).

$$\sigma_{cw} = 0.34 \sigma_B \qquad (3)$$

For the composites and aluminum alloys data derived the lower side from linear relation for HTTM steels. The difference of the slope on the relation between the fatigue strength and tensile strength may be attributed to the difference of the crystallographic structures between steel and aluminum alloys. The fatigue strength estimated at the volume fraction of 0.3 was about 310MPa. This value is comparable or superior to that for Ti-6Al-4V alloys annealed(about 200MPa obtained under a stress ratio of o[10]). On the other hand, for SiCp/A356 composite fish eye failure was frequently observed on the fatigue fracture surface as mentioned in the following section. In case of high strength steels the fish eye failure occurred in the long life range and the fatigue strength was lower than that for surface failure[11]. It is suggested that it would be useful to reduce the shrinkage hole introduced by casting process in order to improve the fatigue strength for SiCp/A356 composites.

3.4 Fractography

Figure 6 shows the microfractographs of tensile fracture surfaces for SiCw/Al2024 and SiCp/A356 composites. The equiaxed dimple patterns are clearly observed on the surface for SiCw/Al2024 composite and dimple sizes are very small up to about 1.0 μm in diameter as shown in Fig. 6(a). A observation at higher magnification revealed the projection of SiC whiskers at the bottom of dimples. On the other hand, for SiCp/A356 composites the SiC particles are found on the fracture surface , while those particles fractured are not observed as indicated in Fig. 6(b). At lower magnification, the SiC whiskers rich regions were frequently observed. It is suggested that the tensile

cracks will start at the SiC whiskers rich regions of the specimens.

Figure 7(a) exhibits the stage I fatigue crack inclined to the load axis of about 40 degree around region of crack initiation for SiCw/Al2024 composite, though the micro holes were rarely observed. Fatigue striation patterns and fine dimples patterns were also found in the crack propagation region(as shown in Fig. 8). The area fraction of striation patterns were very few. It is suggested that the fatigue striation patterns would be formed in the matrix region as shown in Fig. 1(a). For SiCp/A356 composites the fatigue crack initiated at shrinkage hole beneath the specimen surfaces. Moreover, the cracks initiated at the shrinkage holes sited at the interior of specimen as shown in Fig. 7(b). That fish eye failure was observed for SiCp/A356 composites in spite of the volume fraction. The average size of the shrinkage was about 40μm. In the region of fatigue crack propagation the striation patterns were frequently observed and SiC particles were also found. Near the final failure surface the particles were frequently observed. It is concluded that for SiCw/Al2024 composite the fatigue crack would initiate by stage I mechanisms and propagate by striation mechanism, while for SiCp/A356 composite the crack is initiated at the shrinkage hole sited beneath the specimens surfaces or at the interior of specimen.

Mode I crack depth, a_i, and the depth at the onset of fast fracture, a_f were measured and the maximum stress intensity factor, K_{max}, was calculated. Figure 9 shows the relationship between K_{max} and the volume fraction of SiC whiskers or SiC particulates. The region drown by slant lines shows Mode I fatigue crack propagation region where tends to be narrow with the increase of the volume fraction. It is concluded that it is necessary to clear the fatigue crack initiation mechanism in order to analyze the fatigue properties of aluminum composites reinforced by SiC whiskers or SiC particulates.

4. Conclusions

1) Tensile strength of 10 % SiC whiskers reinforced Al2024 composite was about 30 % higher than that of matrix alloy. Tensile strength of that composite was estimated by the equation proposed by Fukuda et al. For SiC particles reinforced A356 composite tensile strength increased at Vf=10 %, while those values saturated at Vf=20 %. Modulus increased with increasing the volume fraction of SiC whiskers or particles, while ductility decreased due to the addition of the SiC whiskers or SiC particles. SEM observation revealed that the crack would propagate to SiC-whiskers/matrix or SiC-particles/matrix interface.

2) The fatigue strength of SiCw/Al2024 composite increased about 65 % in comparison with the matrix alloy. On the other hand, for SiCp/A356 composite the fatigue strength tended to reach the maximum value at the volume fraction of SiC particles of 10 %. The maximum value of fatigue strength was about 30 % increase in comparison with AC4CH wrought aluminum alloy (referred to A356 aluminum alloy). Fatigue crack was initiated by stage I mechanism for SiC whiskers reinforced composite, while for SiC particles reinforced composites fatigue cracks initiated at the shrinkage holes beneath the specimen surfaces (fish eye failure). Fatigue crack propagated by striation mechanism for those composites. The fatigue strength estimated at Vf=30% SiC whiskers was comparable or superior to that of Ti-6Al-4V alloys annealed fabricated by powder metallurgy. For SiCp/A356 composite it is suggested that the reduction

of shrinkage hole introduced during casting process prevented from fish eye failure and improved the fatigue strength.

5 Acknowledgment

Authors thank Tokai carbon Ltd. for the preparation of SiCw/Al2024 aluminum composite used in this study.

Reference

1) A. P. Divecha, S. G. Fishman and S. D. Karmarkar, J. Met., Sep. (1981)12.
2) T. G. Neih and R. F. Karlak, J. Mat. Sci. Letter, 2(1983)119.
3) R. J. Lederich and S. M. L. Sastry, Mat. Sci. Eng., 55(1982) 143.
4) D. F. Hasson, S. M. Hover and C. R. Crowe, J. Mat. Sci., 20(1985)4154.
5) D. Webster, Met. Trans., 13A(1992)1511.
6) D. L. McDanels, Met. Trans., 16A(1985)1105.
7) S. V. Nail, J. K. Tein and R. C. Bates, Int. Met. Rev., 20(1985)275.
8) H. Fukuda and Tsu-Wei Chou, J. Mat. Sci., 17(1982) 1003.
9) M. Fukazawa(Tokai Carbon Co. Ltd.), Private communication.
10) A. Atens, W. Hoffelner, T. W. Duering and J. E. Allison, Scripta Met., 17 (1983)601.
11) C. Masuda, Y. Tanaka, and S. Nishijima, Trans. JSME, 52(1985)847(in Japanese).
12) AA Standard, (1986)
13) A. Sato and R. Mehrabian, Met. Trans., 7B(1976)443.
14) J. Shang, W. Yu and R. O. Ritchie, Mat. Sci. Eng., 102A(1988)181.
15) NRIM Fatigue Data Sheet Technical Document, No. 1(1981).

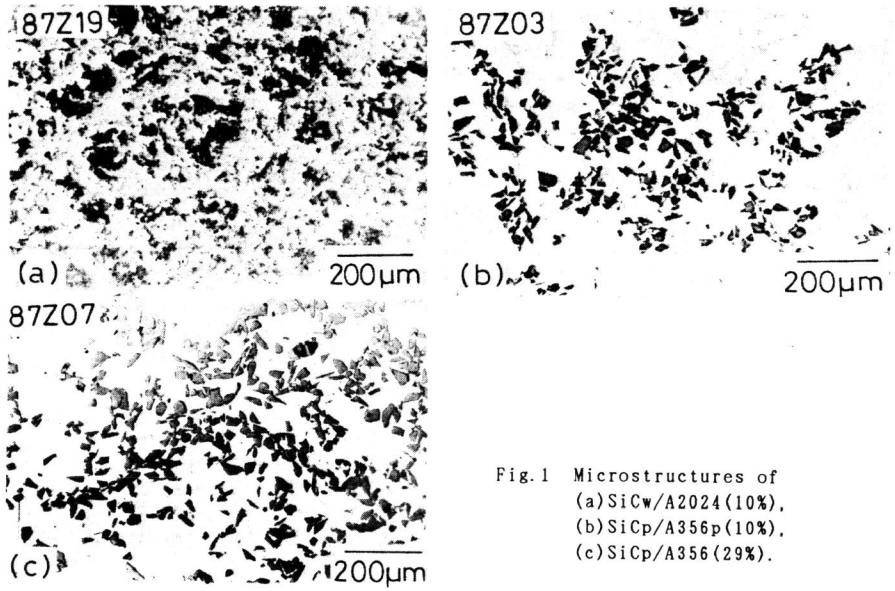

Fig. 1 Microstructures of (a)SiCw/A2024(10%), (b)SiCp/A356p(10%), (c)SiCp/A356(29%).

Table 1 Tensile properties

Material	Thermal treatment	0.2% yield stress (MPa)	Tensile strength (MPa)	Elongation (%)	Young's modulus (GPa)
SiCw/A2024 (10%)	Fab.	221	407	2.6	89
	T6	408	630	4.3	92
SiCp/A356 (10%)	Fab.	103	193	9.2	80
	T6	353	387	2.2	76
SiCp/A356 (20%)	Fab.	125	190	4.5	92
	T6	370	394	0.8	96
A2024 [9]	T6	390	480	10.4	75
A356 [12]	T6	206	284	10	–
AC4CH	T6	215	275	6.9	–

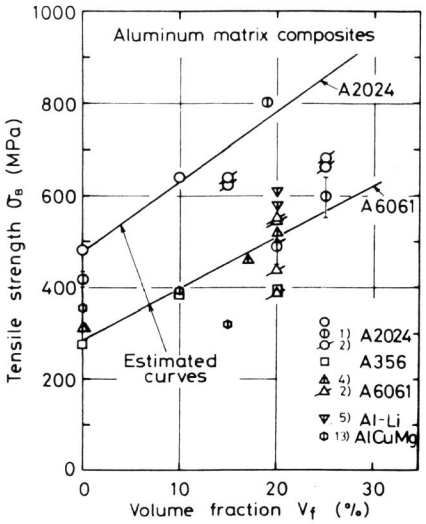

Fig. 2 Relationship between the tensile strength and the volume fraction of SiC whiskers or SiC particles.

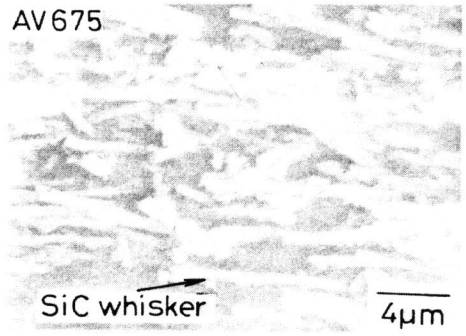

Fig. 3 Microstructure of SiC whiskers contained in SiCw/A2024 composite.

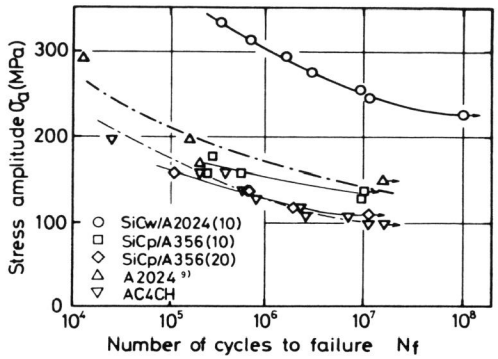

Fig. 4 S-N diagram of SiC reinforced composites and wrought aluminum alloy.

Table 2 Fatigue strength (MPa)

Material	10^5	10^6	10^7
SiCw/A2024 (10%)	380	303	251
SiCp/A356 (10%)	178	152	132
SiCp/A356 (20%)	161	127	105
A2024 [9]	207	164	153
A356 [12]	–	–	90
AC4CH	128	105	101

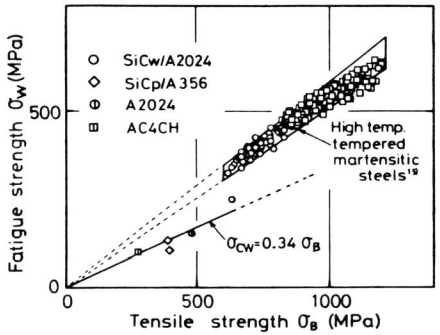

Fig. 5 Relationship between the fatigue strength at 10^7 and the tensile strength.

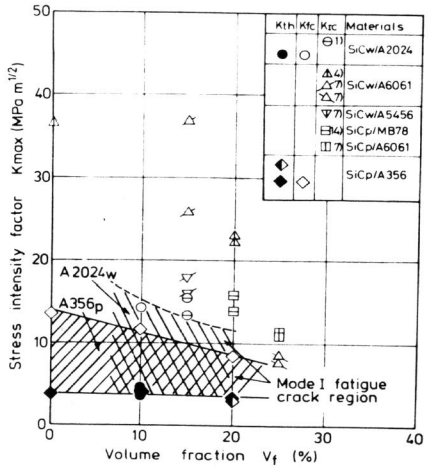

Fig. 9 Relationship between maximum stress intensity factor and the volume fraction.